THE ASTROPHYSICAL JOURNAL, 279:673-678, 1984 April 15

INTERSTELLAR ABSORPTION LINES IN THE INFRARED SPECTRUM OF NGC 2024 IRS 2

JOHN H. BLACK[1,2,3] AND S. P. WILLNER[1,2]

Received 1983 July 11; accepted 1983 October 12

ABSTRACT

A high-resolution infrared spectrum of NGC 2024 IRS 2 shows strong interstellar absorption lines in the $v = 2\text{–}0$ band of CO. A temperature $T = 44^{+1}_{-8}$ K and column density $N(\text{CO}) = 8^{+9}_{-0.8} \times 10^{18}$ cm^{-2} can be inferred from the data. The bulk of the molecular gas in this line of sight has a very small velocity dispersion, $\Delta V \leq 1.45$ km s^{-1}. The observations provide the first sensitive, direct limit upon the CO abundance in a molecular cloud: $CO/H_2 > 8.2 \times 10^{-5}$, a value that is only barely consistent with some values adopted in the recent literature. Broad Brackett-γ emission observed from NGC 2024 IRS 2 is interpreted as being due to a thermally excited stellar wind with an inferred mass loss rate of $3 \times 10^{-7}\ M_{\odot}$ yr^{-1}. A derived upper limit on the stellar temperature of 20,000 K is further evidence against IRS 2 being the exciting star for NGC 2024.

Subject headings: infrared: spectra — interstellar: abundances — interstellar: matter — interstellar: molecules

I. INTRODUCTION

The existence of interstellar molecules was first established by the identification of narrow absorption lines of CH, CH^+, and CN superposed upon the visible spectra of background stars. Until recently, optical absorption-line studies of interstellar matter have been confined primarily to the relatively transparent diffuse interstellar clouds, which are not fully molecular. It is now possible to study genuine molecular clouds by optical absorption-line techniques (Cohen 1973; Crutcher 1980, 1983; Hobbs, Black, and van Dishoeck 1983). It is also feasible to extend such investigations into the infrared. Kleinmann *et al.* (1978) searched unsuccessfully for interstellar absorption lines in the 2 μm spectrum of the highly reddened supergiant Cyg OB2 no. 12. Hall *et al.* (1978) observed infrared lines of interstellar CO in the spectrum of the Becklin-Neugebauer source in the Orion Molecular Cloud. More recently, Scoville *et al.* (1983) have studied in detail both the circumstellar and interstellar absorption in the infrared spectrum of the Becklin-Neugebauer source.

This paper presents initial results of a program to observe infrared interstellar absorption lines. The background star in this work is the infrared point source IRS 2 in NGC 2024 (Grasdalen 1974; Frey *et al.* 1979; Thompson, Thronson, and Campbell 1981). The combination of high foreground extinction, $E(B-V) = 4\text{–}14$ mag, and a relatively large apparent brightness in the infrared ($K = 4.5$, $L = 2.5$) make this star an excellent subject for high-resolution interstellar line spectroscopy in the 2–4 μm wavelength region. The principal goals of this investigation were to measure lines of the ^{12}CO and ^{13}CO $v = 2\text{–}0$ vibration-rotation band and to search for lines of the H_2 $v = 1\text{–}0$ quadrupole vibration-rotation band. Absorption lines of ^{12}CO arising in the eight lowest rotational levels were observed. Level populations and column densities can be derived from the observations. In combination with our upper limit upon the strengths of H_2 lines, it is possible to establish by direct observation a significant lower bound on the CO/H_2 abundance ratio.

II. OBSERVATIONS

Observations were made of the infrared spectrum of NGC 2024 IRS 2 on 1983 February 19, 20, and 21, using the Fourier transform spectrometer (FTS) at the coudé focus of the Kitt Peak 4 m telescope. The instrument is described in detail by Hall *et al.* (1979). Observing began in the late afternoon and continued until just before local midnight. Two InSb detectors were used; the difference in their outputs represented the interferometric signal and the sum, a photometric signal. The ratio of the difference to the sum was recorded as the interferogram, thereby canceling seeing fluctuations and guiding errors (Hall *et al.* 1979). A filter that transmitted from 4100 to 5000 cm^{-1} was used to isolate the regions of the CO and H_2 lines. We also attempted to observe the H_3^+ line at 2691.444 cm^{-1} (Oka 1980, 1981) with a separate pair of detectors, but the signal-to-noise ratio was much lower than expected, and no useful data were obtained.

The source IRS 2, which is invisible at wavelengths less than 1 μm, was centered in one of the 3"8 apertures by peaking up on the photometric DC signal in the K band. Between interferometer scans, the telescope was switched to move the source from one aperture to the other, a separation of 50". Interferograms were also recorded for Sirius to provide a reference atmospheric absorption spectrum and for a tungsten filament to calibrate the response of the system. The total amount of usable data on the source consisted of 81 interferometer scans for a total of 11.55 hours of integration time.

The interferograms were transformed to power spectra for us by Dr. K. P. Hinkle of the Kitt Peak staff using standard procedures. The unapodized resolution of the spectra was 0.020 cm^{-1}, which corresponds to a velocity resolution of 1.4 km s^{-1} in the vicinity of the CO $v = 2\text{–}0$ lines. Data on the three nights were separately corrected for atmospheric absorption by comparison with the Sirius spectra. In order to

[1] Visiting Astronomer, Kitt Peak National Observatory, which is operated by the Association of Universities for Research in Astronomy, Inc., under contract with the National Science Foundation.

[2] Harvard-Smithsonian Center for Astrophysics.

[3] Steward Observatory, University of Arizona.

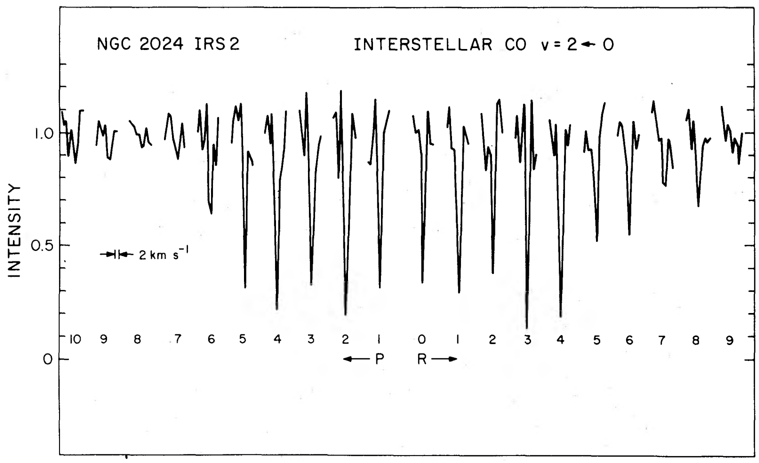

FIG. 1.—The interstellar absorption lines of the CO $v = 2$–0 vibration-rotation band in the spectrum of NGC 2024 IRS 2. Only a small frequency interval around each line is shown. Lines are labeled according to the rotational quantum number of the lower state for the *P*-branch on the left side and the *R*-branch on the right side. A velocity width of 2 km s^{-1} is indicated. Because of the large velocity shift, the corresponding telluric CO lines lie outside the frequency intervals shown.

facilitate the search for narrow spectral features, the continua were made flat by dividing by the calibration lamp spectra and multiplying by a blackbody function. The frequency scales of the spectra were verified by locating narrow atmospheric absorption lines. Finally, the three spectra were combined with weights proportional to their respective signal-to-noise ratios.

When the corrected spectra from all three nights are combined, the maximum signal-to-noise ratio is S/N $\approx$ 14 per resolution element in regions that are free of atmospheric features. The corresponding minimum detectable equivalent width of a narrow line is $W_{\min} \approx 0.0014$ cm^{-1} at the level of 1 standard deviation (1 σ).

A number of interstellar absorption lines in the $v = 2$–0 band of ^{12}CO appear in the spectrum. We refer to the principal isotopic species without a superscript in what follows. The observed profiles from the combined spectrum are shown in Figure 1. Table 1 summarizes the measured equivalent widths of these lines, W_ν in cm^{-1}, together with the rest frequencies $\tilde{\nu}$ (cm^{-1}) in vacuum (Mantz and Maillard 1974) and the adopted oscillator strengths (Kirby-Docken and Liu 1978). Uncertainties in W_ν at the 2 σ level are tabulated, and upper limits are 3 σ. Our observations were made near the time when the Earth's orbital motion produces the maximum redshift along the line of sight to NGC 2024. Typically, the interstellar CO lines were redshifted from the corresponding atmospheric CO lines by 50 km s^{-1}, and corrections applied for atmospheric extinction changed the equivalent widths by less than their measurement uncertainties.

None of the interstellar CO lines are significantly broader than the instrumental width; thus the line width (full width at half-maximum) is $\Delta V \lesssim 1.4$ km s^{-1}. The mean radial velocity of the absorbing gas is determined to be $V_{\rm lsr} = 9.9 \pm 0.4$ km s^{-1}, in harmony with that of the principal velocity component seen in microwave absorption lines ($V_{\rm lsr} \approx 9.5$ km s^{-1}, see § III).

The only other prominent feature in the spectrum is a stellar hydrogen Brackett-γ emission line. The profile of this line is shown in Figure 2, together with the best fitting Gaussian function. The line has a full width at half-maximum of $\Delta V = 137 \pm 16$ km s^{-1} and an equivalent width $|W_\nu| = 0.76 \pm 0.14$ cm^{-1}, and is centered at $V_{\rm lsr} = 17.5 \pm 5.8$ km s^{-1}. No other stellar lines are obviously present. In particular, the He I

TABLE 1

INTERSTELLAR ABSORPTION LINES OF CO $v = 2$–0

	R-BRANCH			*P*-BRANCH			
J	$\tilde{\nu}$ (cm^{-1})	$f(10^{-8})$	W_ν (cm^{-1})	$\tilde{\nu}$ (cm^{-1})	$f(10^{-8})$	W_ν (cm^{-1})	$N_J(10^{18}$ cm$^{-2})$
0.........	4263.83734	7.513	0.019 ± 0.002	...	...	...	0.48
1.........	4267.54195	5.041	0.024 ± 0.002	4256.21760	2.472	0.020 ± 0.004	1.36
2.........	4271.17708	4.567	0.020 ± 0.004	4252.30270	2.947	0.026 ± 0.005	1.53
3.........	4274.74037	4.378	0.023 ± 0.004	4248.31800	3.138	0.022 ± 0.004	1.34
4.........	4278.23459	4.285	0.024 ± 0.002	4244.26430	3.233	0.024 ± 0.003	1.56
5.........	4281.65708	4.235	0.021 ± 0.003	4240.14020	3.286	0.018 ± 0.004	1.02
6.........	4285.00851	4.209	0.014 ± 0.002	4235.94740	3.316	0.011 ± 0.003	0.50
7.........	4288.29000	4.197	0.008 ± 0.003	4231.68555	3.331	0.003 ± 0.002	0.18
8.........	4291.50010	4.194	0.008 ± 0.002	4227.35431	3.338	≤0.005	≤0.20
9.........	4294.63799	4.198	≤0.005	4222.95415	3.340	≤0.008	≤0.12
10........	4297.70500	4.206	≤0.006	4218.48582	3.337	≤0.006	≤0.16
						Total J = 0–7	8.0

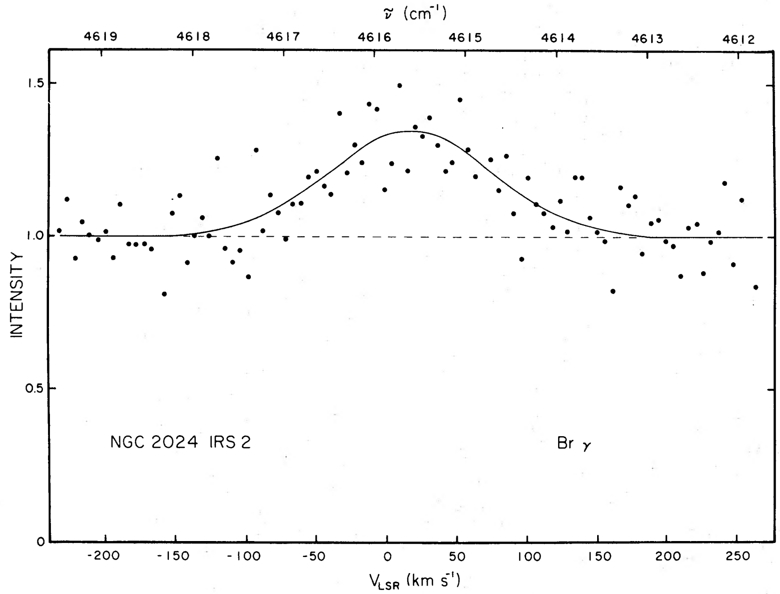

FIG. 2.—The region of the stellar Brγ line in NGC 2024 IRS 2. The data have been smoothed by averaging over four resolution elements. The solid curve is the best fitting Gaussian profile function plus continuum offset. The velocity scale is appropriate for a rest frequency of 4616.55 cm^{-1}.

2^1S–2^1P transition at 4857.454 cm^{-1} is not present with an equivalent width greater than 0.14 cm^{-1}. Several other He I lines arising in $n = 4$ levels were also searched for and not found.

III. DISCUSSION

a) *Molecules*

The infrared observations reported above provide important information on molecular abundances and excitation, and they complement radio frequency emission-line data in useful ways. The absorption-line technique is limited to lines of sight through interstellar clouds that happen to lie toward suitable background stars. The blessing that follows from this constraint is that the background star subtends an effectively infinitesimal solid angle on the sky. Thus, in contrast to most radio emission-line observations, infrared absorption-line studies sample cloud structure and velocity dispersion in one dimension only. Abundances of different molecules observed through absorption lines necessarily refer to the same absorbing column. With infrared techniques, it is possible to observe molecular lines that arise in a number of rotational levels in a single observation. The relative populations can be determined directly and accurately (in principle, at least) and can be used as diagnostics of temperature and density. In NGC 2024, the reliably measured CO lines are sufficiently strong and narrow to be saturated; thus curve-of-growth effects must be taken into account in their analysis. In principle, the column density N_J in each lower level $J \neq 0$ and the Doppler broadening parameter $b = \Delta V/1.665$ km s^{-1} can be determined from the measured strengths of each pair of R-branch and P-branch lines with a common lower state. In practice, the signal-to-noise ratio of our spectra is too low for this direct analysis to yield meaningful results.

The simplest approach to interpretation is to use curves of growth, computed for various values of the Doppler parameter b, to determine a column density N_J from each measured equivalent width. With the assumption of a fixed value of the rotational excitation temperature T_{rot},

$$N_J \propto (2J + 1) \exp(-E_J/kT_{rot}) , \quad (1)$$

where E_J is the excitation energy of rotational level J. The slope of the curve [log $N_J/(2J + 1)$] versus E_J provides a value of T_{rot}. The thermal population distribution that best fits the observed equivalent widths has $b = 0.75$ km s^{-1} (i.e., $\Delta V = 1.25$ km s^{-1}), an excitation temperature $T_{rot} = 44$ K, and a total CO column density $N(CO) = 8.0 \times 10^{18}$ cm^{-2}. It is possible to estimate the range of uncertainty in the derived result as follows. The observed line widths imply an upper limit on the dispersion of $b = 0.87$ km s^{-1}. The curve of growth with that Doppler parameter gives $T_{rot} = 45$ K and $N(CO) = 7.2 \times 10^{18}$ cm^{-2}. The smallest Doppler parameter that gives results consistent with the data is $b = 0.5$ km s^{-1}, for which $T_{rot} = 36$ K and $N(CO) = 1.7 \times 10^{19}$ cm^{-2}. Any thermal distribution with $b < 0.5$ km s^{-1} is excluded by the data. In summary, we find $36 \leq T_{rot} \leq 45$ K, $7.2 \times 10^{18} \leq N(CO) \leq 17 \times 10^{18}$ cm^{-2}, and $0.83 \leq \Delta V \leq 1.45$ km s^{-1}. The inferred values of N_J for the best fitting population distribution are presented in the last column of Table 1.

Any uncertainty in oscillator strength contributes negligibly to the uncertainty in derived column density. The adopted theoretical oscillator strengths for $v = 2$–0 (Kirby-Docken and Liu 1978) are 14% smaller than those that would be derived from the experimental dipole moment function of Kirschner *et al.* (1977). Another recent theoretical calculation (Werner 1981) yields results intermediate between the experimental and our adopted values. These differences can be taken as an indication of the uncertainty in the absolute oscillator strength. Relative oscillator strengths of individual lines within the band should be accurate to the number of significant figures quoted in Table 1.

Thermal population distributions (i.e., T_{rot} = constant) fit the observed data well. For comparison, we have also computed statistical equilibrium excitation models of a 10 level CO molecule using an escape probability treatment of the radiative transfer in the rotational transitions. Only collisions with H_2 were considered. The excitation rates were derived from the He-CO collisional excitation rates of Green and Chapman (1978), scaled for the smaller reduced mass of the H_2-CO system. The excitation models can be used to predict the equivalent widths of the vibration-rotation lines for a variety of values of b, N(CO), density $n(H_2)$, and kinetic temperature T. The observed results can be reproduced with the values of b and N(CO) inferred above as long as the density is at least $n(H_2) \gtrsim 1000$ cm^{-3}. At such densities, the excitation temperature is constant for $J \leq 6$ and is equivalent to the kinetic temperature. The predicted optical depths of the $J = 1$–0, 2–1, and 3–2 rotational lines are 79, 262, and 422 respectively, at the preferred values of the line width and total column density. For comparison, the line center optical depths of the strongest infrared absorption lines are $\tau \approx 1$–5, and corrections for saturation are much less severe.

The expected positions of the $v = 2$–0 lines of ^{13}CO (Chen, Rao, and McDowell 1976) were searched carefully, and no lines were detected. The P and R branch lines with $J \leq 4$ all show $W_\nu < 0.006$ cm^{-1} (3 σ). The most sensitive limit is provided by $W_\nu < 0.0033$ cm^{-1} (3 σ) for the $R(2)$ line. The $v = 2$–0 oscillator strengths of ^{13}CO are 0.935 times the corresponding values in ^{12}CO; thus, $N_J(^{13}CO) < 8.7 \times 10^{16}$ cm^{-2} for $J = 2$. For a uniform excitation temperature $T_{rot} = 44$ K, the corresponding limit on the total column density is $N(^{13}CO) < 4.2 \times 10^{17}$ cm^{-2}, so that $N(CO)/N(^{13}CO) > 17$.

We are able to place interesting limits upon the strengths of two quadrupole vibration-rotation lines of H_2, $v = 1$–0 $S(0)$ and $S(1)$. The rest frequencies were taken from Bragg, Brault, and Smith (1982). No feature exceeding 1.5 σ appears near the expected Doppler-shifted frequencies. The 3 σ upper limits for the $S(0)$ and $S(1)$ lines are $W_\nu < 0.0061$ and $W_\nu < 0.016$ cm^{-1} respectively. The oscillator strengths of these lines are $f = 9.37 \times 10^{-14}$ and 5.46×10^{-14}, respectively, based on the transition probabilities of Turner, Kirby-Docken, and Dalgarno (1977). Thus, the column density of H_2 in $J = 0$ is $N_0(H_2) < 7.3 \times 10^{22}$ cm^{-2}, and in $J = 1$, is $N_1(H_2) < 3.2 \times 10^{23}$ cm^{-2}.

Our most sensitive limit on molecular hydrogen is that on the column density in the $J = 0$ level. It is likely that the $J = 0$ and $J = 1$ populations are thermalized (Dalgarno, Black, and Weisheit 1973). Thus, if we assume that the derived excitation temperature of CO is equal to that for H_2, we conclude that $N(H_2) < 8.8 \times 10^{22}$ cm^{-2} at $T \leq 45$ K. This implies a lower bound on the CO/H_2 abundance ratio in the NGC 2024 molecular cloud of $N(CO)/N(H_2) > 8.2 \times 10^{-5}$. If the carbon abundance is solar (Lambert 1978), more than 1/12 of the carbon must be in CO.

A brief discussion of the importance of *direct* measurements of the CO/H_2 ratio is in order (see Lequeux 1981 for a recent review of indirect determinations). The CO abundance in molecular clouds must be accurately determined if reliable conclusions are ever to be drawn from CO rotational line data concerning the molecular content of the Milky Way and other galaxies. Our direct limit is barely consistent with the indirect determination, CO/$H_2 \approx 8.5 \times 10^{-5}$, of Frerking, Langer, and Wilson (1982) for the interiors of the ρ Oph and Taurus dark clouds. If the abundance ratio of the ^{12}C and ^{13}C isotopic species is CO/^{13}CO ≤ 90, then our abundance limit implies $H_2/^{13}CO < 1.1 \times 10^6$. This limit is comfortably larger than the value 4×10^5 adopted by Blitz and Shu (1980) but is only marginally consistent with values as large as 10^6 (e.g., Solomon, Scoville, and Sanders 1979).

Our limit on the CO abundance in a quiescent molecular cloud is consistent with CO abundances that have been determined for regions of shock-heated molecular gas. Storey *et al.* (1981) analyzed far-infrared emission lines and inferred CO/$H_2 \approx (1.1$–$2.2) \times 10^{-4}$ for the shocked gas in the Orion Molecular Cloud. Such abundance determinations are model dependent, but for the Orion Molecular Cloud the models that are used to derive the abundances are highly constrained (McKee *et al.* 1982; Chernoff, Hollenbach, and McKee 1982).

A number of atoms and molecules have been observed in the NGC 2024 cloud at radio frequencies. Radio absorption-line measurements have been made of OH (Goss *et al.* 1976), H_2CO (Genzel *et al.* 1979), and atomic H (Lockhart and Goss 1978). The column densities of these species in the 9.5 km s^{-1} velocity component are 1.8×10^{15} cm^{-2}, 1.8×10^{13} cm^{-2}, and 1.7×10^{21} cm^{-2} respectively. The absorbing column in the direction of the NGC 2024 thermal radio continuum source is probably similar to that sampled by our infrared observations of the highly obscured star IRS 2; however, it must be remembered that the absorbing cloud shows considerable structure on angular scales less than or comparable to the extent of the radio continuum source (Lockhart and Goss 1978; Fomalont and Weliachew 1973). The microwave absorption lines exhibit widths $\Delta V \approx 1.5$ km s^{-1} in harmony with those of the narrow infrared lines of CO.

If we assume that the infrared and microwave absorbing columns are directly comparable, then we find column-averaged abundance ratios of OH/CO $= 2 \times 10^{-4}$ and H_2CO/CO $= 2 \times 10^{-6}$. Our observations provide an interesting direct limit on the relative abundance of atomic hydrogen in a molecular cloud, $N(H)/N(H_2) > 0.019$, which is somewhat larger than the values inferred by indirect means for several dark clouds (e.g., McCutcheon, Shuter, and Booth 1978; Snell 1981). Such a large atomic fraction might reflect an unusually high dissociation rate or unusually inefficient H_2 formation if the atoms and molecules are coextensive. Alternatively, the atoms and molecules might occupy different strata in the cloud, so that the relatively large column density of H would indicate the presence of a substantial atomic envelope (Wannier, Lichten, and Morris 1983). In either case, the H/H_2 column density ratio is a crucial property to be explained by future theoretical models of the NGC 2024 cloud.

Several rotational transitions of CO have been observed in emission (Plambeck and Williams 1979; Phillips *et al.* 1979; Loren *et al.* 1981; Koepf *et al.* 1982). The temperature $T = 45$ K inferred from these observations (e.g., Plambeck and Williams 1979) agrees well with that derived from our infrared observations. The $J = 1$–0 and 2–1 lines of all observed isotopic species of CO are considerably broader than the infrared absorption lines and peak at radial velocities that are 1–2 km s^{-1} higher. This discrepancy can most easily be understood by noting that the core of the NGC 2024 molecular cloud is offset somewhat from the line of sight to

IRS 2 and that the large antenna beams of the radio frequency studies average over a cloud of complex structure. The total CO column density estimated from radio line observations, $N(\mathrm{CO}) = 1.5 \times 10^{19}$ cm^{-2} (Phillips *et al.* 1980) is within a factor of 2 of our preferred value for the line of sight to IRS 2 and is within the range of uncertainty allowed by our data. One point deserves special emphasis in this connection: our observations demonstrate that a substantial column density of CO in this cloud has a much smaller velocity dispersion than would be inferred from observations of the radio emission lines. Further observations will be required to establish whether this might be a property of giant molecular clouds in general and to suggest what effects this might have on the interpretation of widespread CO line emission observed with relatively poor angular resolution.

b) *Stellar Features*

The only prominent stellar feature in our spectrum of IRS 2 is the H Brγ line in emission. A Gaussian profile with a peak intensity 1.34 times that of the adjacent continuum fits the observed line well. There is no indication of a narrow, purely nebular component of the Brγ line. Thompson, Thronson, and Campbell (1981) observed several Brackett lines at lower spectral resolution in an 8″ beam centered on IRS 2. They assumed an intrinsic Brackett decrement given by case B recombination and used the apparent Brackett decrement to infer an extinction $A_V = 12 \pm 3$ mag to the emitting region. Their observed Brγ flux of 2.7×10^{-12} ergs cm^{-2} s^{-1} and continuum flux density of 9 Jy at $\tilde{\nu} = 4615$ cm^{-1} yield an equivalent width of $|W_\nu| = 1.0$ cm^{-1}. Within our 2 σ uncertainties, this equivalent width agrees with our measurement of the broad emission line seen in a 3″.8 beam.

The broad Brackett-γ emission is most likely due to a thermally excited stellar wind, as discussed by Krolik and Smith (1981). Emission in local thermodynamic equilibrium (LTE) might approximate the line ratios emitted by a dense circumstellar wind. At 20,000 K, the LTE Brackett line ratios are indistinguishable from those produced by recombination at $T = 10{,}000$ K, provided the extinction is the same in both cases. The Brγ flux, corrected for extinction corresponding to $A_V = 12$ (Thompson, Thronson, and Campbell 1981) implies a mass loss rate of 3×10^{-7} $M_\odot$ yr^{-1} (Krolik and Smith 1981, eq. [17]). The absence of stellar helium lines, especially 2^1S–2^1P, lends further support to the hypothesis that IRS 2 is some sort of Be star rather than an O type star, which would be necessary to photoionize the NGC 2024 H II region.

The K magnitude of IRS 2 and the luminosity of the region NGC 2024 can be combined to yield an upper limit on the temperature of the region of IRS 2 that produces the 2 μm radiation. This region is likely to be the stellar photosphere to be consistent with the observed reddening and the long-wavelength energy distribution. For a blackbody that radiates in the Rayleigh-Jeans regime at a wavelength λ,

$$T_{\mathrm{eff}}^3 = 4.59 \times 10^{11} \frac{F}{F_\lambda} \left(\frac{\lambda}{\mu\mathrm{m}}\right)^{-4} . \qquad (2)$$

Here $F = \int_0^\infty F_\lambda \, d\lambda$ and F_λ is the flux density per micron. The presence of Brγ emission shows that IRS 2 is relatively hot, and the Rayleigh-Jeans approximation should be reasonable at 2.2 μm. If IRS 2 is indeed associated with NGC 2024 so that all of its radiation is converted to the infrared, the upper limit for F is the integrated flux from the entire region, 7.1×10^{-9} W m^{-2} (derived from Table 3 of Harper 1974). The 2.2 μm flux density corrected for the extinction derived by Thompson, Thronson, and Campbell (1981) is about 1.7×10^{-11} W m^{-2} μm^{-1}. Thus, $T_{\mathrm{eff}} < 20{,}000$ K. If, instead, all of the flux from IRS 2 were included in the 50″ beam of Thronson *et al.* (1978), the upper limit would be 10,000 K.

The absolute magnitude of IRS 2 places it well into the range of supergiants. For the temperatures of interest, $-0.8 \lesssim (V-K)_0 \lesssim 0$ (Johnson 1966). A distance modulus of 8.5 (500 pc) gives $M_K = -5.1$ and M_V between -5 and -6, much too bright for a giant but a bit fainter than the early supergiants listed by Panagia (1973). It is thus possible that the distance to IRS 2 is up to a factor of 2 greater than assumed, and IRS 2 might simply be a background star. Other stars of the Orion OB1 association show a range of distances up to at least 800 pc (Humphreys 1978). If IRS 2 is indeed a background star, the upper limit on its temperature need not apply because there would not necessarily be enough surrounding dust to convert most of the stellar luminosity into far-infrared radiation. In any case, IRS 2 is unlikely to be the principal exciting star of NGC 2024. Thompson, Thronson, and Campbell (1981) reached the same conclusion from considerations of heating and ionization.

The radial velocity difference of 12.5 ± 6 km s^{-1} between the stellar hydrogen emission line and the radio recombination lines (Krügel *et al.* 1982) could be taken as further evidence that IRS 2 is not associated with the H II region. However, a velocity difference of similar size between the circumstellar emission of the Becklin-Neugebauer source and the surrounding molecular cloud (Scoville *et al.* 1983) suggests that such discrepancies may be possible.

IV. CONCLUSIONS

Our observations of the infrared spectrum of NGC 2024 IRS 2 demonstrate the utility of absorption-line techniques for investigating molecular clouds. Measurements of vibrational lines of interstellar CO provide information on its abundance and excitation and on conditions in the cloud. Perhaps the most significant conclusion of this work is that we are on the threshold of being able to observe H_2 directly in thick molecular clouds. In the future, it should be possible to determine the CO abundance accurately by direct observation in a few clouds. The limit on CO/H_2 implied by the present data is already comparable to some values adopted in the literature. Infrared absorption-line techniques can also provide the ideal means of studying nonpolar molecules such as C_2H_2 and CH_4 which lack dipole-allowed radio frequency spectra.

We are very grateful that Kitt Peak National Observatory can maintain an instrument as complex and delicate as the FTS for use by visiting astonomers. Thanks to Dr. K. P. Hinkle and the rest of the Kitt Peak staff, our observing was fruitful and the data reduction was relatively painless. We thank R. I. Thompson, P. T. P. Ho, E. F. van Dishoeck, J. H. Krolik, N. Z. Scoville, and C. H. Townes for helpful comments on the manuscript. J. H. B. was supported by the National Science Foundation through grant AST 81-14718 to Harvard University.

REFERENCES

Blitz, L., and Shu, F. H. 1980, *Ap. J.*, **238**, 148.
Bragg, S. L., Brault, J. W., and Smith, W. H. 1982, *Ap. J.*, **263**, 999.
Chen, D.-W., Rao, K. N., and McDowell, R. S. 1976, *J. Molec. Spectrosc.*, **61**, 71.
Chernoff, D. F., Hollenbach, D. J., and McKee, C. F. 1982, *Ap. J.* (*Letters*), **259**, L97.
Cohen, J. G. 1973, *Ap. J.*, **186**, 149.
Crutcher, R. M. 1980, *Ap. J.*, **239**, 549.
———. 1983, preprint.
Dalgarno, A., Black, J. H., and Weisheit, J. C. 1973, *Ap. Letters*, **14**, 77.
Fomalont, E. B., and Weliachew, L. 1973, *Ap. J.*, **181**, 781.
Frerking, M. A., Langer, W. D., and Wilson, R. W. 1982, *Ap. J.*, **262**, 590.
Frey, A., Lemke, D., Thum, C., and Fahrbach, U. 1979, *Astr. Ap.*, **74**, 133.
Genzel, R., Downes, D., Pauls, T., Wilson, T. L., and Bieging, J. 1979, *Astr. Ap.*, **73**, 253.
Goss, W. M., Winnberg, A., Johansson, L. E. B., and Fournier, A. 1976, *Astr. Ap.*, **46**, 1.
Grasdalen, G. L. 1974, *Ap. J.*, **193**, 373.
Green, S., and Chapman, S. 1978, *Ap. J. Suppl.*, **37**, 169.
Hall, D. N. B., Kleinmann, S. G., Ridgway, S. T., and Gillett, F. C. 1978, *Ap. J.* (*Letters*), **223**, L47.
Hall, D. N. B., Ridgway, S., Bell, E. A., and Yarborough, J. M. 1979, *Proc. Soc. Photo-Opt. Instrum. Eng.*, **172**, 121.
Harper, D. A. 1974, *Ap. J.*, **192**, 557.
Hobbs, L. M., Black, J. H., and van Dishoeck, E. F. 1983, *Ap. J.* (*Letters*), **271**, L95.
Humphreys, R. M. 1978, *Ap. J. Suppl.*, **38**, 309.
Johnson, H. L. 1966, *Ann. Rev. Astr. Ap.*, **4**, 309.
Kirby-Docken, K., and Liu, B. 1978, *Ap. J. Suppl.*, **36**, 359.
Kirschner, S. M., LeRoy, R. J., Ogilvie, J. F., and Tipping, R. M. 1977, *J. Molec. Spectrosc.*, **65**, 306.
Kleinmann, S. G., Hall, D. N. B., Ridgway, S. T., and Wright, E. L. 1978, *A.J.*, **83**, 373.
Koepf, G. A., Buhl, D., Chin, G., Peck, D. D., Fetterman, H. R., Clifton, B. J., and Tannenwald, P. E. 1982, *Ap. J.*, **260**, 584.
Krolik, J. H., and Smith, H. A. 1981, *Ap. J.*, **249**, 628.
Krügel, E., Thum, C., Martin-Pintado, J., and Pankonin, V. 1982, *Astr. Ap. Suppl.*, **48**, 345.
Lambert, D. L. 1978, *M.N.R.A.S.*, **182**, 249.
Lequeux, J. 1981, *Comments Ap.*, **9**, 117.
Lockhart, I. A., and Goss, W. M. 1978, *Astr. Ap.*, **67**, 355.
Loren, R. B., Plambeck, R. L., Davis, J. H., and Snell, R. L. 1981, *Ap. J.*, **245**, 495.
Mantz, A. W., and Maillard, J.-P. 1974, *J. Molec. Spectrosc.*, **53**, 466.
McCutcheon, W. H., Shuter, W. L. W., and Booth, R. S. 1978, *M.N.R.A.S.*, **185**, 755.
McKee, C. F., Storey, J. W. V., Watson, D. H., and Green, S. 1982, *Ap. J.*, **259**, 647.
Oka, T. 1980, *Phys. Rev. Letters*, **45**, 531.
———. 1981, *Phil. Trans. Roy. Soc. London, A*, **303**, 543.
Panagia, N. 1973, *A.J.*, **78**, 929.
Phillips, T. G., Huggins, P. J., Kuiper, T. B. H., and Miller, R. E. 1980, *Ap. J.* (*Letters*), **238**, L103.
Phillips, T. G., Huggins, P.J., Wannier, P. G., and Scoville, N. Z. 1979, *Ap. J.*, **231**, 720.
Plambeck, R. L., and Williams, D. R. W. 1979, *Ap. J.* (*Letters*), **227**, L43.
Scoville, N. Z., Kleinmann, S. G., Hall, D. N. B., and Ridgway, S. T. 1983, *Ap. J.*, **275**, 201.
Snell, R. L. 1981, *Ap. J. Suppl.*, **45**, 121.
Solomon, P. M., Scoville, N. Z., and Sanders, D. B. 1979, *Ap. J.* (*Letters*), **232**, L89.
Storey, J. W. V., Watson, D. M., Townes, C. H., Haller, E. E., and Hansen, W. L. 1981, *Ap. J.*, **247**, 136.
Thompson, R. I., Thronson, H. A., Jr., and Campbell, B. G. 1981, *Ap. J.*, **249**, 622.
Thronson, H. A., Jr., Harper, D. A., Keene, J., Loewenstein, R. F., Moseley, H., and Telesco, C. M. 1978, *A.J.*, **83**, 492.
Turner, J., Kirby-Docken, K., and Dalgarno, A. 1977, *Ap. J. Suppl.*, **35**, 281.
Wannier, P. G., Lichten, S. M., and Morris, M. 1983, *Ap. J.*, **268**, 727.
Werner, H.-J. 1981, *Mol. Phys.*, **44**, 111.

J. H. BLACK: Steward Observatory, University of Arizona, Tucson, AZ 85721

S. P. WILLNER: Harvard-Smithsonian Center for Astrophysics, 60 Garden Street, Cambridge, MA 02138